applied sciences

MDPI

Article

On the Detection and Removal of Oxides from Laser Treated Surfaces

Jiří Matějíček [1,*], Jiří Martan [2], Denys Moskal [2], Ole Peters [3], Sebastian Kraft [3], František Lukáč [1], Michal Hajíček [4], Vlastimil Brožek [1], Udo Löschner [3] and Jörg Schille [3]

[1] Institute of Plasma Physics of the Czech Academy of Sciences, U Slovanky 1a, 18200 Praha, Czechia; matejicek@ipp.cas.cz, lukac@ipp.cas.cz, brozek@ipp.cas.cz
[2] New Technologies Research Centre, University of West Bohemia, Univerzitní 8, Plzeň, 30100, Czechia; jmartan@ntc.zcu.cz , moskal@ntc.zcu.cz
[3] Laserinstitut Hochschule Mittweida, University of Applied Sciences Mittweida, Technikumplatz 17, Mittweida, 09648, Germany; ollimacp@gmail.com, kraft@hs-mittweida.de, loeschne@hs-mittweida.de, schille@hs-mittweida.de
[4] UJP Praha, Nad Kamínkou 1345, 156 00 Praha, Czechia; hajicek@ujp.cz
* Correspondence: matejicek@ipp.cas.cz

Abstract: Laser texturing is a technique of surface modification widely applicable in various industrial areas, for example as a substrate pre-treatment for thermal spray coatings. When performed in air, the elevated surface temperature may induce oxidation of the metallic surfaces, which in turn may undermine the coating adhesion. The degree of oxidation depends on the substrate material as well as the processing parameters. This brings about the need for analyzing the oxide amount as well as its removal if needed. In the current study, the applicability of two widely available methods for oxide analysis – x-ray diffraction (XRD) and energy-dispersive spectrometry (EDS) is investigated and compared. Furthermore, three types of oxide removal methods – annealing in a reducing atmosphere, gentle laser ablation and acid etching – were applied and their efficiency was demonstrated on three classes of materials – stainless steel, W-based and Ti-based materials. Oxide removal by laser ablation was additionally analyzed and correlated with in-process fast heat accumulation temperature measurement.

Keywords: laser texturing; oxidation; thermal spraying; oxide detection; oxide removal; laser cleaning, temperature measurement

Citation: To be added by editorial staff during production.

Academic Editor: Firstname Lastname

Received: date
Revised: date
Accepted: date
Published: date

1. Introduction

Laser surface texturing is a widespread surface modification technology that involves altering the surface properties of a material by modifying its texture and roughness with high-intensity laser beams. The laser-material interaction phenomena may include localized melting, vaporization or ablation [1]. As a result of these processes, microscopic patterns such as dimples, grooves, pillars or other shapes can be formed with high flexibility, accuracy and reproducibility. Laser surface texturing can be applied on a wide range of materials, spanning metals, ceramics, polymers and so on. The surface modifications can be directed towards improvement in friction properties [2,3,4], erosion resistance [5], wettability [6], hydrophobicity or hydrophilicity [1,3,7], performance in biomedical applications (such as osseointegration and cell adhesion) [8], corrosion resistance [7], light absorption [9] or enhanced adhesion of thermal spray coatings [10,11,12,13].

When the laser processing of metallic materials is carried out in air (which may be needed for example in high-rate processing [12], where the complex instrumentation would make a vacuum enclosure too demanding) the elevated surface temperatures may

lead to oxidation. This in turn can affect the functional properties of the surface. For example, in thermal spray coatings, oxides on the substrate hinder the formation of a metallurgical bonding between metallic coating and metallic substrate [14,15], leading to a reduced adhesion. On the other hand, the adhesion of oxide ceramic coating may be enhanced by suitable substrate oxidation [16]. In other applications, laser-induced oxidation of the final metallic surface is carried out on purpose, e.g. to improve the corrosion resistance [17,18] or to provide localized electrical insulation in biomedical applications [19]. Oxidation may also play a role in the formation of so-called laser-induced periodic surface structures [20].

Therefore, there is a need for oxide content control on the laser treated surfaces. This in turn entails its detection (and qualitative or quantitative evaluation) and – where undesirable – removal. In this work, the applicability of two commonly available analytical techniques – EDS and XRD – for a comparative/semi-quantitative determination of oxide content on representative laser treated materials is investigated. A simplified practical method that circumvents the complications associated with non-ideal samples and allows a semi-quantitative comparison of the oxide content after different variants of the laser treatment is proposed. Furthermore, three techniques for reducing the oxides, namely heat treatment in a reducing atmosphere, moderate laser ablation and acid etching are applied. The efficiency of these methods is evaluated.

2. Materials and Methods

Three types of materials were used for the testing, all of them as substrates for laser texturing as a pre-treatment for thermal spraying. These were AISI 304 stainless steel and W-based materials (pure W and W-Cu composite with ~39vol% Cu) as substrates for plasma sprayed W coatings for potential use in plasma-facing components in fusion reactors, and Ti6Al4V alloy as a substrate for plasma sprayed Ti for orthopedical implants.

On the W-based materials, laser texturing was performed with a nanosecond (ns) laser (YLP-HP, wavelength 1070 nm, max. optical power 200 W; IPG Photonics, USA), creating a hexagonal dimple pattern. The dimples had 30 μm depth, 30 μm width and 50 μm spacing. Besides the same dimple pattern, the steel samples were textured by a continuous wave (cw) fiber laser (YLR-3000-SM, wavelength 1070 nm, max. optical power 3000 W; IPG Photonics, USA), forming grooves of 25 μm depth and 70 μm distance in parallel or perpendicular orientation. On the Ti alloy, again a dimple pattern was formed by a nanosecond laser, with 55 μm depth, 50 μm width and 70 μm spacing.

Surface morphology was observed by scanning electron microscope (SEM) EVO MA15 (Carl Zeiss SMT, Oberkochen, Germany). EDS was carried out in the same microscope, using a Quantax system with XFlash 5010 detector (Bruker, Berlin, Germany). EDS measurements were performed at 500x magnification (to encompass a number of the surface texture features), 8.5 mm working distance, 1 nA emission current and 10 kV acceleration voltage. XRD was carried out using D8 Discover diffractometer (Bruker, Karlsruhe, Germany). Phase analysis was performed with full profile Rietveld refinement using TOPAS 5 software.

Annealing for oxide removal on the W-based materials was performed in a furnace filled with hydrogen at 800 °C for 1 hour (similar treatment was used previously to clean W powder from oxides accumulated by long term storage [21]). Acid etching of the W-Cu composite material was performed by soaking the samples in 40% hydrofluoric acid (HF) for 20, 40 and 60 s (similar to treatment used in [22]). Surface cleaning by 'gentle ablation' with ultra-short laser pulses and low pulse energies was carried out with a femtosecond slab laser (FX 200, wavelength 1030 nm, average power 80 W, pulse duration 650 fs; Edgewave GmbH, Würselen, Germany) at a variety of conditions. On the W-Cu composite material, frequency of the laser pulses was varied between 6 and 24 MHz, traverse velocity was varied between 30 and 480 m/s and number of passes between 1 and 3 (specific parameter combinations will be mentioned below together with the results). On the Ti alloy, only the 10 MHz at 100 m/s combination was used.

Fast temperature measurement during laser ablation was done by LabIR Ultrashort measurement system [23]. InGaAs detector with 5 MHz bandwidth was used for detection of infrared (IR) radiation through the polygon scanning head [24]. As the pulse repetition frequency was higher than detector bandwidth (6 to 24 MHz compared to 5 MHz), the effect of separate laser pulses was not resolved and only average value of heat accumulation was evaluated. To decrease noise, averaging from many laser scanning lines was done (from 412 to 7, depending on the scanning speed from 30 to 480 m/s). The calibration to obtain temperature values from voltage was done by static heating using small heating element and measuring through the scan head.

3. Results

3.1. General approach

It should be noted that the results presented below are semi-quantitative only. The samples have significant surface roughness (which is the main purpose of laser texturing), the amount of oxides on the surface is fairly small and their thickness may vary between the valleys and ridges of the patterns. Precise EDS analysis relies on the assumption of a smooth surface and homogeneous distribution of the present elements within the gauge volume. Moreover, oxygen is detected on practically every sample that was exposed to air. Also, the x-ray intensity of lighter elements is lower than of the heavier ones. The roughness and spatial distribution present a similar complication for the XRD analysis. Thus, the samples are far from ideal case [25,26,27]. Therefore, the general approach is to determine the oxides semi-quantitatively by measurements on a) a pristine sample (i.e. freshly ground metal) and b) sample(s) oxidized by a known process. This way, a practical boundary between a 'clean' and 'oxidized' surface can be determined, specific for each material. For materials with the same type of morphology, at least a qualitative comparison of the degree of oxidation among treatments with different parameters can be obtained.

3.2. Oxide analysis

Representative morphologies of the laser textured steel, W, W-Cu and Ti alloy substrates are shown in Figs. 1-4. These give an idea of the size of the texture features (grooves, dimples) as well as the nature of the various surfaces. The deeper regions of the grooves and dimples are typically smooth with occasional molten droplets. On the steel substrates treated by the cw laser, the ridges have similar appearance. In contrast, in the dimple pattern textures formed by the ns laser, the upper regions have more complex morphology and typically contain a significant amount of fine particles. These likely originate from the ejection from the depth and redeposition on the top surface. These regions are likely to experience a higher degree of oxidation, due to higher specific surface. Minor differences in morphology obtained by similar laser patterns on different materials, can be also observed. Parts of Figs. 2-4 also show the surface morphologies after distinct post-treatments; their effects will be discussed in section 3.3.

Results of the EDS analysis on the W-based materials are shown in Table 1. In addition to clean and laser treated samples, another example of oxidized surface - treated by electric discharge machining (EDM) - is included. One can see a clear distinction between the values obtained on significantly oxidized (LST), moderately oxidized (EDM) and clean (ground) surfaces. Similar results from the steel samples are summarized in Table 2. The overall oxygen content is generally lower and the difference between oxidized and clean surface is less distinct. Yet a boundary value between these two may be established. Such a result could be expected in view of the surface morphology, where the steel exhibited much cleaner surfaces than the W-based materials, however, this is a rather indirect indicator. On these materials, XRD measurement was also attempted, however, the oxide amount was found to be below the detection limit.

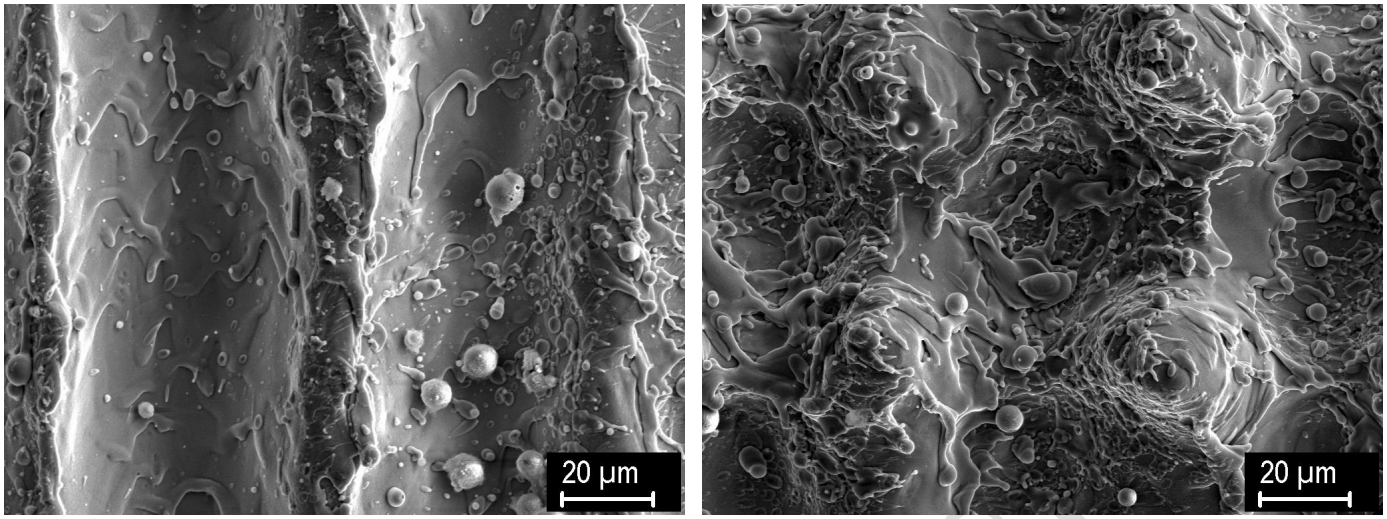

(**a**) (**b**)

Figure 1. Surface morphology of steel samples textured with a cw laser. (**a**) Lines with a width of 70 µm and depth of 25 µm; (**b**) Grid of perpendicular lines with a width of 70 µm and depth of 25 µm.

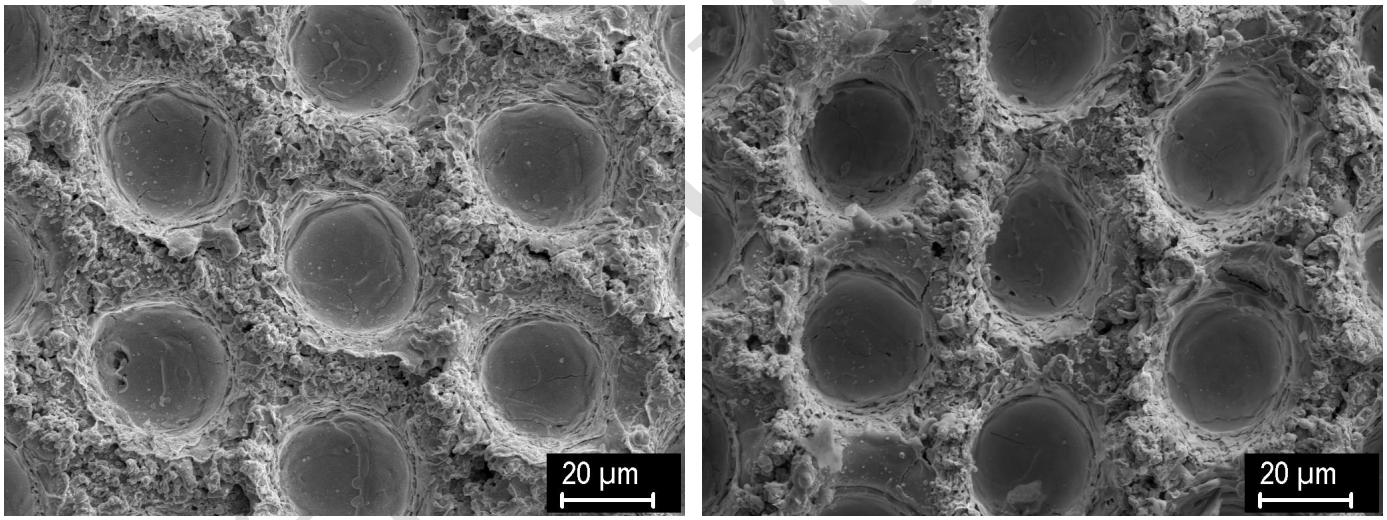

(**a**) (**b**)

Figure 2. Surface morphology of W samples textured with a ns laser, dimple pattern. (**a**) As-textured; (**b**) heat-treated in hydrogen atmosphere.

Table 1. EDS results on W-based samples; 'ground' represents a clean sample, 'dimples' and 'EDM' represent samples oxidized by laser texturing and EDM.

Sample	O (wt%)	Sample	O (wt%)
WCu (ground)	0.9	W (ground)	1.6
WCu (dimples)	10.2	W (dimples)	12.2
WCu (EDM)	6.5	W (EDM)	4.6

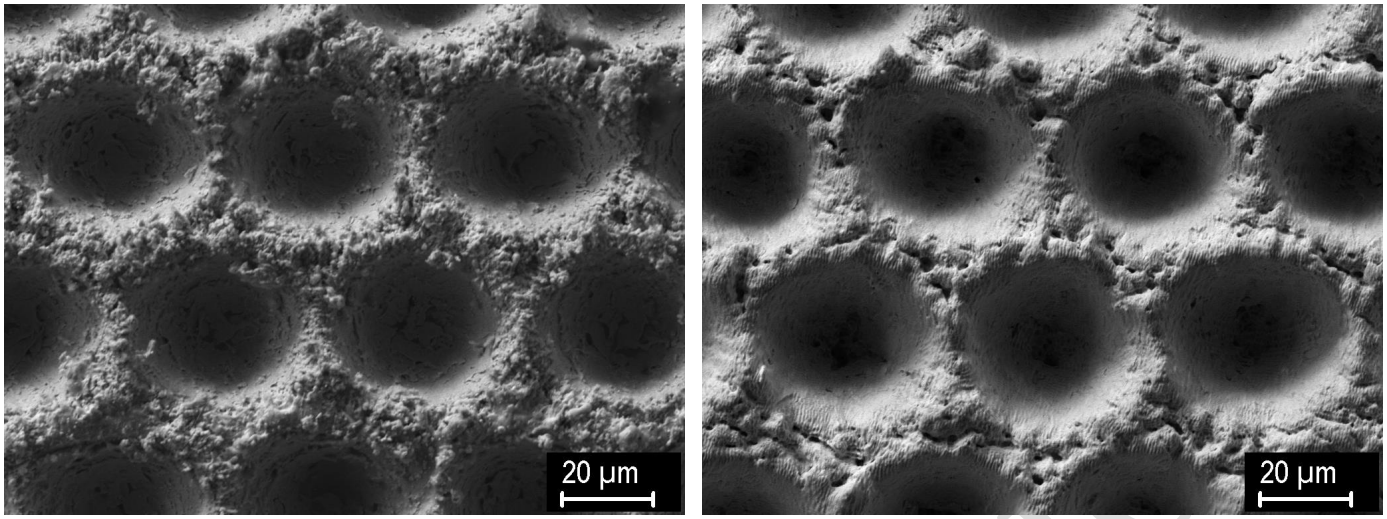

(**a**) (**b**)

Figure 3. Surface morphology of W-Cu samples textured with a ns laser, dimple pattern. (**a**) As-textured; (**b**) after laser cleaning with gentle ablation (6 MHz, 30 m/s, 3 passes).

Results obtained on Ti alloy samples after three types of treatment are shown in Table 3. The oxygen content as determined by EDS in the three variants of laser texturing (regular, with N_2 shielding and with subsequent laser cleaning by gentle ablation) does not show significant distinction with respect to the processing variant. However, there are marked differences between the results from the LST surfaces, a clean one (freshly ground) and a significantly oxidized one (long-term storage in open air). The XRD results show similar values of the oxide content in the regular and N_2-shielded LST samples, but a significantly reduced one in the sample treated by gentle ablation. Apparently, in this case the analytical technique was able to better distinguish the laser processing variants. While there is not a tight correlation between the EDS and XRD results, both techniques show marked distinction between the clean, moderately oxidized and heavily oxidized samples. While the EDS provides compositional information based on individual elements, the XRD provides information based on crystallographic phases. In this case, the oxide phase was identified as corundum phase (Al_2O_3). In literature, the oxidation products of Ti6Al4V alloy were typically Ti-based [28,29,30] or a mixture of Ti- and Al-based oxides [31,32,33]. However, these cases mostly concerned isothermal oxidation, while the process during laser ablation is highly dynamic. Moreover, a fraction of the oxide scale present before the laser treatment may have been retained, due to different ablation thresholds of the oxide and the base metal. Also, the XRD is not particularly sensitive to small variations in elemental compositions, so the possibility of the corundum phase containing Ti, Al and V elements cannot be ruled out.

Table 2. EDS results on steel samples. 'Ground' represents a clean sample, 'grid', 'lines' and 'dimples' represent samples oxidized by variants of laser texturing.

Sample	O (wt%)
Steel (ground)	1.7-2.1
Steel (grid)	2.9
Steel (lines)	3.9
Steel (dimples)	3.5

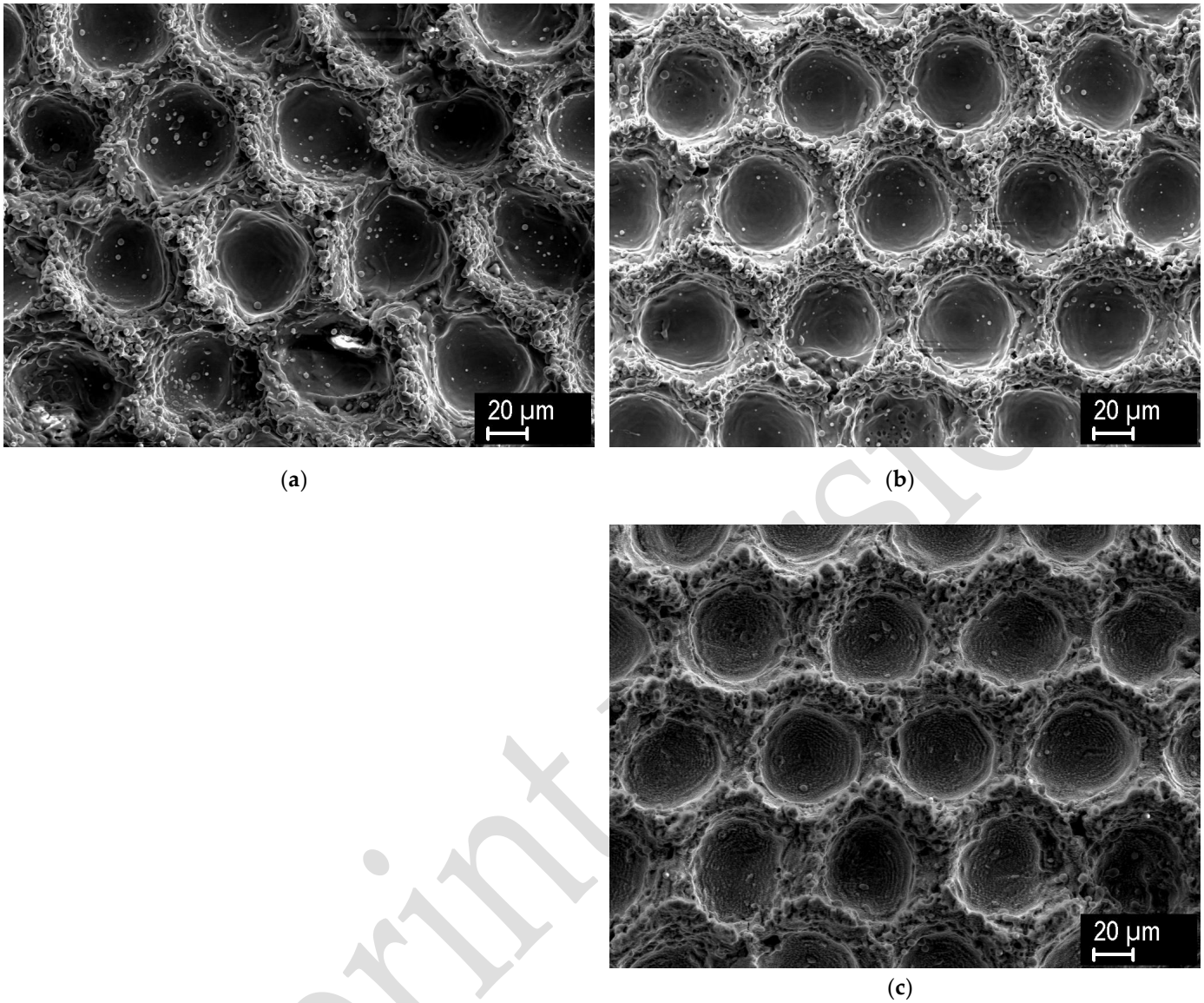

(**a**) (**b**)

(**c**)

Figure 4. Surface morphology of Ti alloy samples textured with a ns laser, dimple pattern. (**a**) Regular texturing; (**b**) texturing with nitrogen shielding; (**c**) texturing with subsequent gentle ablation.

Table 3. EDS and XRD results on Ti alloy samples; 'ground' represents a clean sample, three lines with 'dimples' represent samples oxidized by variants of laser texturing, 'grit-blasted + storage' represents an example of significantly oxidized sample (initially treated by grit blasting, then stored a long time in open air).

Sample	O (wt%)	oxide (wt%)
Ti (ground)	0.6	0
Ti (dimples)	11-12	17.9
Ti (dimples + N2 shielding)	13-15	18.1
Ti (dimples + laser cleaning)	11-12	2.4
Ti (grit-blasted + storage)	31	52.9

A short note on the experimental scatter concerning the values presented in Tables 1-6: For the EDS values, obtained with the current setup, typical standard deviations were in the range 10-15% of the presented value; for the XRD values, it was around 1% (absolute value). These numbers refer to a single measurement; on top of this, a spatial variation from place to place may be considered. When such variation was observed with a non-

negligible extent, ranges from several measurements are shown. In this regard, it should be noted that the XRD data were taken from a much larger area – ~3 cm^2, compared to 1.1 mm^2 for EDS.

3.3. Oxide removal

EDS results from W-based samples treated by annealing in hydrogen atmosphere are shown in Table 4. For both materials, the oxygen content was significantly reduced with respect to the laser treated surface. However, the process appears to be more efficient for the WCu sample, where the content was comparable to a clean sample, while for the 100% W sample, it was still slightly higher. As can be seen in Fig. 2, there is no marked effect on the surface morphology.

EDS results from the W-based samples treated by HF etching are presented in Table 5. Compared to the laser treated surface (Table 1), the oxygen content is markedly reduced for all etching times, although still a little higher than for the hydrogen annealing treatment. There is no apparent trend with respect to etching time, thus 20 s immersion appears sufficient to significantly reduce the amount of oxides. Similarly to the previous case, there was no marked effect of this treatment on the surface morphology.

Table 4. EDS results on W-based samples annealed in hydrogen atmosphere.

Sample	O (wt%)
WCu (dimples, annealed)	0.6
W (dimples, annealed)	3.4

Table 5. EDS results on W-based samples treated by HF etching.

Sample	O (wt%)
WCu (dimples, HF 20 s)	1.9
WCu (dimples, HF 40 s)	1.8
WCu (dimples, HF 60 s)	2.8

Table 6. EDS results (in wt% O) on WCu samples treated by gentle laser ablation, along with time resolved temperatures (in °C) measured during the process. Since there were varying combinations of pulse frequency and traverse velocity, and three parameters altogether, their values have to be presented inside the table as well. Bold numbers indicate the parameter values, regular numbers present the oxygen content from EDS (wt%) and heat accumulation temperature (°C) measured by LabIR Ultrashort.

Frequency (MHz)	**No. of passes**	**Velocity (m/s)**		
		30	**60**	**120**
6	**1**	2.1, ---	2.2, 416	2.4, 411
	2	2.3, 415	2.1, 413	3.1, 412
	3	2.3, 413	2.1, 412	2.4, 410
		60	**120**	**240**
12	**1**	2.1, 391	2.6, 387	2.9, 385
	2	2, 385	2.4, 382	2.8, 376
	3	2, 380	2.7, 376	2.6, 375
		120	**240**	**480**
24	**1**	3.6, 365	4.2, 366	5.7, 336
	2	2.9, 356	3.7, 353	5.1, 344

	3	2.6, 340	3.8, 348	4.4, 321
As-textured		9-12		

EDS results from the WCu samples treated by gentle ablation with various parameters are presented in Table 6. The traverse velocity was chosen to obtain the same overlap of laser spots on surface in the same column of the table with changing pulse frequency. In the first column the distance of laser spot centers is 5 μm (overlap 87%), in the second column 10 μm (overlap 75%), in the last column 20 μm (overlap 50%). So in each column the material surface gets the same number of laser pulses, but with different pulse energy and in different time interval. With increasing frequency, the pulse energy is decreased (to have the same average power) and time of treatment is shortened. From the obtained results, one can make several observations. The effectiveness of oxide removal generally depends on the laser treatment parameters. For the high frequency and high traverse velocity ranges, the degree of oxide removal increases with a number of passes. At the same time, it increases with decreasing velocity. For the lowest frequency (6 MHz), the oxide removal is the most effective, while the other two parameters do not have any pronounced effect. Even the least intense treatment (24 MHz, 480 m/s, 1 pass) resulted in noticeable oxide reduction. Such treatment also has an effect on the surface morphology, as shown in Fig. 3. Comparison of Fig. 3a (as-textured surface) and 3b (treated with gentle ablation at the most intense setting) reveals that the major geometrical features of the texture are preserved, while only the micromorphology is affected. Specifically, the microroughness on the texture ridges is partially smoothed. In this figure only the most diverse examples are shown, while at other parameter combination, intermediate effects were observed.

The heat accumulation temperatures measured during the gentle pulsed laser ablation are shown in Table 6. Although intuitively the heat accumulation should increase with increasing pulse repetition frequency, as mentioned e.g. in [34], in this case the observed temperatures decreased with increasing frequency. It is due to the decrease of pulse energy with increase of frequency, while having the same pulse overlap.

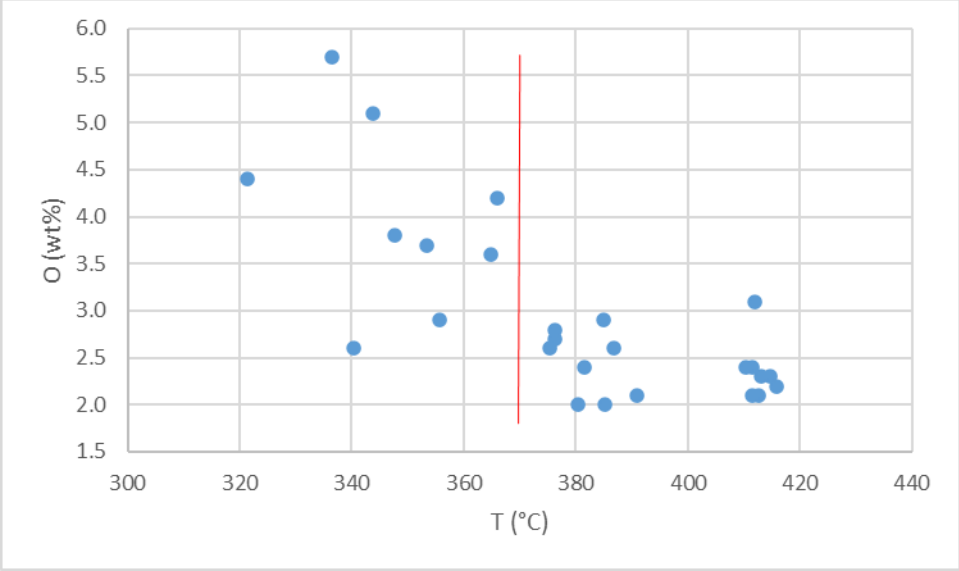

Figure 5. Correlation of oxide content after laser cleaning with heat accumulation temperature during laser cleaning. Indicated is value of 370 °C as a transition from partial to full oxide removal.

When analyzing correlation of oxide content with heat accumulation temperature (Fig. 5), interesting result is found. At temperatures higher than ~370 °C the oxide is removed completely and at low temperatures the removal is only partial and the oxide values are scattered. The ablation is done in short time (hundreds of picoseconds to units of

nanoseconds) after the femtosecond laser pulses and the measured temperature is the heat accumulation in hundreds of nanoseconds. But anyway the process seems to be governed by thermal effects, as was observed for similar process (cleaning, polishing) by laser ablation of AM1 superalloy [35], where the change of the process was found in similar temperature range, from 325 to 405 °C of calculated heat accumulation. In this case, the increase of repetition frequency also led to a decrease of heat accumulation temperature. The scatter of the oxygen values on left side of Fig. 5 (high frequency, 24 MHz) is due to different number of passes. When repeating the laser process, the oxides on the surface are partially removed in each pass, but the heat accumulation should stay the same. The measured difference in heat accumulation can be due to change of emissivity caused by oxides removal. This does not happen for lower frequencies, where the oxides are removed already in the first pass.

4. Conclusions

The presence/absence or quantity of oxides on laser textured metallic materials can be beneficial or detrimental, depending on specific application. From this stems the need for oxide detection and control. In this work, two methods for the analysis of oxygen/oxide content - EDS and XRD - were applied on three classes of industrially relevant materials. While there are other techniques suitable for this purpose (e.g. X-ray photoelectron spectroscopy [18,25], Raman spectroscopy [20,25], Auger electron spectroscopy [25] or secondary ion mass spectroscopy [25]), this work focused on two techniques widely available in materials laboratories. The laser textured surfaces present a non-ideal case for such analysis, due to surface roughness and inhomogeneous spatial distribution of the species in the gauge volume, besides the oxides being present in small quantities. Therefore, fully quantitative evaluation was not attempted. Instead, a simplified practical approach was taken, providing relative, semi-quantitative results. By comparison of results on pristine samples and those oxidized by a known process, a distinct boundary between 'clean' and 'oxidized' surfaces can be established, specific for each material. For materials with the same type of morphology and measured in the same setup, a relative comparison of the degree of oxidation among treatments with different parameters may be obtained. This can then be used as feedback for the laser treatment process – selection of specific process parameters, process modification, or for a decision whether a dedicated post-treatment is necessary. The applicability of this procedure using EDS was successfully demonstrated on stainless steel, W and WCu composite and Ti alloy. For XRD, the oxide content in the investigated steel and W-based materials was below the detection limit; useful results were obtained only on the Ti alloy. Thus, for these small oxide contents, XRD turned out to be applicable only on a limited range of materials. Also, the nature of the information provided by these techniques differs. While EDS determines the fraction of oxygen as an element, XRD yields a fraction of the oxide as a phase, with the added benefit of identifying the phase's structure.

Three techniques of oxide removal were also investigated – annealing in a reducing atmosphere, acid etching and 'gentle' laser ablation. On W-based materials, all three methods were proven to be effective in oxide removal. For the gentle laser ablation, a dependence of the results on several process parameters, namely the pulse frequency, traverse velocity and number of passes, was found. The heat accumulation temperature measurements revealed a threshold value of ~370 °C below which the oxide content values were scattered and above which the oxide was removed in a stable manner. Besides the effect on oxide content, the chosen parameters also affected the micromorphology of the textured surface, which can have an influence on the coating adhesion as well. The other two methods did not affect the micromorphology significantly. The selection of a given method would be governed by their availability, effectiveness in oxide removal, experimental demands, effects on micromorphology, etc., while all these aspects would have to be evaluated for a specific application.

Author Contributions: Conceptualization, J. Mat.; methodology, J.Mat., D.M., J.Mar.; investigation, J.Mat., J.Mar., D.M., O.P., S.K., M.H., F.L., V.B.; writing—original draft preparation, J.Mat., J.Mar.; writing—review and editing, J.Mar., J. Mat.; project administration, J.Mar.; supervision, U.L., J.S.; funding acquisition, J.Mar., J.Mat., U.L., J.S. All authors have read and agreed to the published version of the manuscript.

Funding: Financial support through the project "Advanced coating substrate preparation by shifted and ultrafast laser texturing'' jointly funded by Technology Agency of the Czech Republic (grant no. TH75020001) and Saxon Ministry of the Arts and Science (grant no. 100569490) is gratefully acknowledged. Part of the work devoted to W-based substrates was supported by Technology Agency of the Czech Republic through grant no. TK03030045. The work was also supported by the Ministry of Education, Youth and Sports of the Czech Republic (Programme Johannes Amos Commenius, call Excellent Research, project MEBioSys, No. CZ.02.01.01/00/22_008/0004634, co-funded by EU).

Data Availability Statement: Data supporting the conclusions of this article are available at the following DOI: 10.5281/zenodo.14260651.

Conflicts of Interest: The authors declare no conflicts of interest.

References

1. Kalinowski, A.; Radek, N.; Orman, Ł.; Pietraszek, J.; Szczepaniak, M.; Bronček, J. Laser Surface Texturing: Characteristics and Applications. In Proceedings of the System Safety: Human - Technical Facility - Environment; 2023; Vol. 5, 240–248, doi: 10.2478/czoto-2023-0026
2. Mao, B.; Siddaiah, A.; Liao, Y.; Menezes, P.L. Laser Surface Texturing and Related Techniques for Enhancing Tribological Performance of Engineering Materials: A Review. *J. Manuf. Process.* 2020, *53*, 153–173, doi:10.1016/j.jmapro.2020.02.009
3. Kumar, V.; Verma, R.; Kango, S.; Sharma, V.S. Recent Progresses and Applications in Laser-Based Surface Texturing Systems. *Mater. Today Commun.* **2021**, *26*, 101736, doi:10.1016/j.mtcomm.2020.101736.
4. Schille, J.; Schneider, L.; Mauersberger, S.; Szokup, S.; Höhn, S.; Pötschke, J.; Reiß, F.; Leidich, E.; Löschner, U. High-Rate Laser Surface Texturing for Advanced Tribological Functionality. *Lubricants* **2020**, *8*, 1491–1499, doi:10.3390/lubricants8030033.
5. Wahab, J.A.; Ghazali, M.J. Erosion Resistance of Laser Textured Plasma-Sprayed Al2O3-13%TiO2 Coatings on Mild Steel. *Wear* **2019**, *432–433*, 202937, doi:10.1016/j.wear.2019.202937.
6. Schille, J.; Loeschner, U.; Ebert, R.; Scully, P.; Goddard, N.; Exner, H. Laser Micro Processing Using a High Repetition Rate Femto Second Laser. In Proceedings of the 29th International Congress on Applications of Lasers and Electro-Optics; 2010; Vol. 103, p. 33.
7. Conradi, M.; Kocijan, A.; Klobčar, D.; Godec, M. Influence of Laser Texturing on Microstructure, Surface and Corrosion Properties of Ti-6al-4v. *Metals (Basel).* **2020**, *10*, 1504, doi:10.3390/met10111504.
8. Shivakoti, I.; Kibria, G.; Cep, R.; Pradhan, B.B.; Sharma, A. Laser Surface Texturing for Biomedical Applications: A Review. *Coatings* 2021, *11*, 124. doi:10.3390/coatings11020124
9. Kawaguchi, H.; Yasuhara, R.; Yang, H.; Hori, C.; Miyagawa, R.; Sugioka, K.; Ota, M.; Uehara, H. Femtosecond Vector Vortex Laser Ablation in Tungsten: Chiral Nano-Micro Texturing and Structuring. *Opt. Mater. Express* **2024**, *14*, 424, doi:10.1364/ome.510141.
10. Kromer, R.; Sokołowski, P.; Candidato, R.T.; Costil, S.; Pawłowski, L. Control of the Mesostructure of Suspension Plasma-Sprayed Coating with Laser Surface Texturing: Application to TBC. *J. Therm. Spray Technol.* **2019**, *28*, doi:10.1007/s11666-019-00835-7.
11. Matějíček, J.; Vilémová, M.; Moskal, D.; Mušálek, R.; Krofta, J.; Janata, M.; Kutílek, Z.; Klečka, J.; Heuer, S.; Martan, J.; et al. The Role of Laser Texturing in Improving the Adhesion of Plasma Sprayed Tungsten Coatings. *J. Therm. Spray Technol.* **2019**, *28*, 1346–1362, doi:10.1007/s11666-019-00924-7.
12. Kraft, S.; Peters, O.; Schille, J.; Mušálek, R.; Martan, J.; Dlouhá, Ž.; Klečka, J.; Matějíček, J.; Houdková, Š.; Moskal, D.; et al. High-Speed Laser Surface Structuring for Thermal Spray Coating Preparation. *Phys. Status Solidi A* **2024**, *221*, doi:10.1002/pssa.202300710.
13. Mušálek, R.; Tesař, T.; Minařík, J.; Matějíček, J.; Lukáč, F.; Peters, O.; Kraft, S.; Loeschner, U.; Schille, J.; Dudík, J.; Martan, J. High-Speed Laser Patterning of YSZ Ceramic Substrates for Plasma Spraying: Microstructure Manipulation and Adhesion of YSZ Coatings. *J. Therm. Spray Technol.* **2024**, doi:10.1007/s11666-024-01852-x

14. Lienhard, J.; Crook, C.; Azar, M.Z.; Hassani, M.; Mumm, D.R.; Veysset, D.; Apelian, D.; Nelson, K.A.; Champagne, V.; Nardi, A.; et al. Surface Oxide and Hydroxide Effects on Aluminum Microparticle Impact Bonding. *Acta Mater.* **2020**, *197*, 28–39, doi:10.1016/j.actamat.2020.07.011.
15. Khamsepour, P.; Moreau, C.; Dolatabadi, A. Effect of Particle and Substrate Pre-Heating on the Oxide Layer and Material Jet Formation in Solid-State Spray Deposition: A Numerical Study. *J. Therm. Spray Technol.* **2023**, *32*, 1153–1166, doi:10.1007/s11666-022-01509-7.
16. Omar, N. irinah; Yusuf, Y.; Sundi, S.A. bin; Abu Bakar, I.A.; Andre Fabiani, V.; Abdul Rahim, T.; Yamada, M. Influence of Remaining Oxide on the Adhesion Strength of Supersonic Particle Deposition TiO2 Coatings on Annealed Stainless Steel. *Coatings* **2023**, *13*, 1086, doi:10.3390/coatings13061086.
17. Nánai, L.; Vajtai, R.; George, T.F. Laser-Induced Oxidation of Metals: State of the Art. *Thin Solid Films* **1997**, *298*, 160–164, doi:10.1016/S0040-6090(96)09390-X.
18. Swayne, M.; Perumal, G.; Padmanaban, D.B.; Mariotti, D.; Brabazon, D. Exploring the Impact of Laser Surface Oxidation Parameters on Surface Chemistry and Corrosion Behaviour of AISI 316L Stainless Steel. *Appl. Surf. Sci. Adv.* **2024**, *22*, 100622, doi:10.1016/j.apsadv.2024.100622.
19. Moura, C.G.; Carvalho, O.; Gonçalves, L.M.V.; Cerqueira, M.F.; Nascimento, R.; Silva, F. Laser Surface Texturing of Ti-6Al-4V by Nanosecond Laser: Surface Characterization, Ti-Oxide Layer Analysis and Its Electrical Insulation Performance. *Mater. Sci. Eng. C* **2019**, *104*, 109901, doi:10.1016/j.msec.2019.109901.
20. Segovia, P.; Wong, A.; Santillan, R.; Camacho-Lopez, M.; Camacho-Lopez, S. Multi-Phase Titanium Oxide LIPSS Formation under fs Laser Irradiation on Titanium Thin Films in Ambient Air. *Opt. Mater. Express* **2021**, *11*, 2892–2906, doi:10.1364/ome.431210.
21. Matějíček, J.; Vilémová, M.; Veverka, J.; Kubásek, J.; Lukáč, F.; Novák, P.; Preisler, D.; Stráský, J.; Weiss, Z. On the Structural and Chemical Homogeneity of Spark Plasma Sintered Tungsten. *Metals (Basel).* **2019**, *9*, 879, doi:10.3390/met9080879.
22. Zhang, H.J.; Tian, X. qin; Ding, X.Y.; Zheng, H.Y.; Luo, L.M.; Wu, Y.C.; Yao, J.H. Study on the Effect of Vacuum Fusion Infiltration Technology on the Properties of Tungsten/Copper Joining Interface. *Nucl. Eng. Technol.* **2024**, *56*, 2367–2374, doi:10.1016/j.net.2024.01.048.
23. Measuring system for pulsed laser material processing. Available online: https://ultrashort.labir.cz/
24. J. Martan, D. Moskal, C. Beltrami, M. Honner, I. Ramon-Conde, O. Peters, J. Schille, V. Lang, U. Loeschner, Development of Fast Temperature Measurement System for Ultrashort Pulse Laser Material Processing, Proceedings of Lasers in Manufacturing Conference (LIM 2023), WLT, Munich, 26-29 June 2023
25. *Springer Handbook of Materials Measurement Methods*; Czichos, H., Saito, T., Smith, L., Eds.; Springer, 2006; ISBN 978-3-640-20785-6.
26. Energy Dispersive Spectroscopy (EDS/EDX): An Overview. Available online: https://www.azolifesciences.com/article/Energy-Dispersive-Spectroscopy-(EDSEDX)-An-Overview.aspx
27. How to find which oxides are formed after oxidation or corrosion and how to quantify it? Is it possible to quantify from the EDS elemental analysis? Available online: https://www.researchgate.net/post/How-to-find-which-oxides-are-formed-after-oxidation-or-corrosion-and-how-to-quantify-it-Is-it-possible-to-quantify-from-the-EDS-elemental-analysis
28. Fargas, G.; Roa, J.J.; Sefer, B.; Pederson, R.; Antti, M.L.; Mateo, A. Oxidation Behavior of Ti6Al4V Alloy Exposed to Isothermal and Cyclic Thermal Treatments. In Proceedings of the METAL 2017 - 26th International Conference on Metallurgy and Materials, Brno, Czechia, 2017; 1573–1579.
29. Guleryuz, H.; Cimenoglu, H. Oxidation of Ti-6Al-4V Alloy. *J. Alloys Compd.* **2009**, *472*, 241–246, doi:10.1016/j.jallcom.2008.04.024.
30. Kumar, S.; Sankara Narayanan, T.S.N.; Ganesh Sundara Raman, S.; Seshadri, S.K. Thermal Oxidation of Ti6Al4V Alloy: Microstructural and Electrochemical Characterization. *Mater. Chem. Phys.* **2010**, *119*, 337–346, doi:10.1016/j.matchemphys.2009.09.007.
31. Dong, E.; Yu, W.; Cai, Q.; Cheng, L.; Shi, J. High-Temperature Oxidation Kinetics and Behavior of Ti–6Al–4V Alloy. *Oxid. Met.* **2017**, *88*, 719–732, doi:10.1007/s11085-017-9770-0.
32. Du, H.L.; Datta, P.K.; Lewis, D.B.; Burnell-Gray, J.S. Air Oxidation Behaviour of Ti-6A1-4V Alloy between 650 and 850°C. *Corrosion Sci.* **1994,** *36*, 631-642
33. Estupinán-López, F.; Orquiz-Muela, C.; Gaona-Tiburcio, C.; Cabral-Miramontes, J.; Bautista-Margulis, R.G.; Nieves-Mendoza, D.; Maldonado-Bandala, E.; Almeraya-Calderón, F.; Lopes, A.J. Oxidation Kinetics of Ti-6Al-4V Alloys by Conventional and Electron Beam Additive Manufacturing. *Materials (Basel).* **2023**, *16*, 1187, doi:10.3390/ma16031187.
34. Weber, R.; Graf, T.; Berger, P.; Onuseit, V.; Wiedenmann, M.; Freitag, C.; Feuer, A. Heat Accumulation during Pulsed Laser Materials Processing. *Opt. Express* **2014**, *22*, 11312–11324, doi:10.1364/oe.22.011312.
35. Moskal, D.; Martan, J.; Kučera, M.; Houdková, Š.; Kromer, R. Picosecond Laser Surface Cleaning of AM1 Superalloy. *Physics Procedia* **2016,** *83*, 249–257, doi:10.1016/j.phpro.2016.08.020